Temperature Dependence of Rate Coefficients and Branching Ratios for the NH_2 + NO Reaction via Microcanonical Variational Transition State Theory

Eric W.-G. Diau and Sean C. Smith*

Department of Chemistry, University of Queensland, Brisbane, Qld 4072, Australia

Received: January 30, 1996; In Final Form: May 9, 1996[⊗]

Calculations of the temperature dependence of the rate coefficient and product branching ratios in the NH_2 + NO reaction have been performed using microcanonical varitational transition state theory (μVTST) in conjunction with Rice−Ramsperger−Kassel−Marcus (RRKM) theory. The calculations have utilized parameters from Walch's complete active space self-consistent field (CASSCF)/internally contracted configuration interaction (ICCI) calculations for the stationary points on the potential energy surface, together with simple Morse potentials for the minimum energy pathways of the entrance and the OH exit channels. The computed total rate coefficient (k_{tot}) displays a negative temperature dependent between 300 and 3000 K, in good agreement with the results of direct kinetic measurements. The predicted values of the branching ratio for formation of OH (α) are strongly temperature dependent, increasing rapidly from 0.1 at room temperature to 0.85 at 3000 K. Sensitivity modeling indicates that the enthalpy of the products (HN_2 + OH) is a critical quantity that needs to be determined more accurately in order to make genuinely quantitative predictions.

Introduction

The reaction of the NH_2 with NO plays a key role in the thermal $DeNO_x$ process.[1−4] It is believed that there are two major channels involved in the reaction mechanism:[4]

$$NH_2 + NO \rightarrow HN_2 + OH \quad (1a)$$

$$\rightarrow N_2 + H_2O \quad (1b)$$

Reaction 1a is a radical-generation channel that may contribute to the chain reactions via production of the radical species, whereas reaction 1b is a chain-termination step that produces two stable molecules with exothermicity of 125 kcal mol^{-1}. The kinetics of this reaction has been studied extensively via direct measurements[5−10] as well as kinetic modeling.[3,4,11−13] The temperature dependence of the total thermal rate coefficient (k_{tot}) for this reaction has been recently reported to be in a good agreement among most experiments.[10] However, the branching ratio α, defined as the rate coefficient of reaction 1a divided by k_{tot}, is still a riddle because of the large discrepancies between the results of the direct measurements and the flame combustion modeling.[13] For instance, the value of α is agreed to be ~0.1 at room temperature, and it increases to 0.2 at 620 K, 0.19 at 1000 K, and 0.17 at 1173 K according to the results of laser kinetic measurements by Bulatov et al.,[6] Atakan et al.,[7] and Stephens et al.,[8] respectively. On the other hand, it has been pointed out that such small values of α, when extrapolated to the range of thermal $DeNO_x$ temperatures (1100−1400 K), are not sufficient to account for the current modeling mechanism for the flow reactor data.[3,4] Other modeling studies of the NH_3−NO flame have indicated that α varies with temperature from 0.48 at 1050 K to >0.8 at 1400 K or from 0.5 at 1500 K to 0.8 at 2150 K.[11,12] Recently, Halbgewachs et al.[13] have performed a series of kinetic modeling calculations based on the data obtained from pyrolysis of the NH_3 and NO mixture in a steady reactor. The branching ratio was found to increase rapidly from 0.27 at 950 K to 0.58 at 1273 K, which to some extent provides a bridge between the α values of the direct measurements at lower temperatures and those of the flame modeling at higher temperatures.

With respect to the theoretical investigations of the system, more attention has been paid to reaction 1b over the past decade because of its interesting multiple bond-switching mechanism, i.e., it involves the breaking of all three bonds in the reactants and the formation of three entirely different bonds in the products. Gilbert et al.[14] have evaluated the rate coefficient for reaction 1b using Rice−Ramsperger−Kassel−Marcus (RRKM)/master equation theory with an estimation for the relevant molecular parameters referring to early *ab initio* data.[15,16] They treated the loose transition state for the initial recombination of reactants with a simple Gorin model. However, the extreme anharmonicity inferred for the intermediate appears to have resulted from the simplistic overall reaction mechanism employed as well as the insufficient accuracy of the *ab initio* potential energy surface (PES) and RRKM parameters. Two limiting cases (slow or rapid) for the internal rearrangement of the energetic intermediate were considered in order to interpret the experimental observation of the pressure-independence of k_{tot}. Phillips[17] performed an RRKM calculation for reaction 1b based on an *a priori* capture rate model using a steady-state approximation but eliminating the possibility of collisional stabilization for the energetic intermediates due to the relatively short lifetime of the intermediate species. Two PESs, with associated RRKM parameters, were employed according to the *ab initio* results of Melius and Binkley[18] or Harrison et al.[19] The RRKM results for the two sets qualitatively agreed with those of early experiments at temperatures less than 400 K even if the loose transition state of the simple bond fission channel was not treated variationally. More recently, Diau et al.[10] have carried out a multichannel RRKM calculation including reactions 1a and 1b as well as the collisional deactivation (the latter via a strong collision approximation with a collision efficiency factor) based on high-level multireference PES data calculated by Walch.[20] A negative temperature dependence of k_{tot} was predicted in accordance with most experimental observations. However, the

[⊗] Abstract published in *Advance ACS Abstracts,* June 15, 1996.

S0022-3654(96)00299-7 CCC: $12.00

relevant parameters for the two bond fission transition states were obtained by fitting the values of k_{tot} and α at room temperature with those of experiments. It was pointed out that, according to their modeling, α is very sensitive to the enthalpy of reaction 1a. With incorporation of Troe's simple expression for the collision efficiency (β_c)[21] in the calculation, the total branching ratio of the two collisional deactivation channels was determined to be 0.03 at room temperature, decreasing to be negligible for temperatures greater than 1000 K at 50 Torr pressure.

In view of the previous results from both experimental and theoretical work on the title reaction, one would like a theoretical model for the reaction to address at least the following three features: (1) k_{tot} is relatively large at room temperature ($\sim$1.5 $\times$ 10^{-11} cm^3 molecule^{-1} s^{-1}) and it decreases with increasing temperature, which is normally the case for addition−rearrangement reactions without an intrinsic energy barrier; (2) k_{tot} is pressure-independent from a few Torr to 1 atm, implying (as indicated in the calculations of Phillips[17] and Diau et al.[10]) that the energetic intermediates have a considerably shorter lifetime ($\sim 10^{-11}$ s) with respect to rearrangement than the time between collisions at the pressures and temperatures of interest; (3) α is about 0.1 at room temperature and it increases with increasing temperature. In particular, the variation of α with temperature is not yet clear owing to apparent inconsistencies between the results of direct and indirect experiments.

In order to progress some way toward the resolution of these uncertainties, we have carried out microcanonical variational transition state theory (μVTST)/RRKM calculations for the NH_2 + NO system using computational methodology that we have developed in recent years,[22] based on Walch's PES and molecular parameters.[20] We believe the results reported in this paper provide significant new evidence relating to the temperature dependence of the branching ratio α for this very important reaction.

Computational Details

The calculations for the NH_2 + NO reaction are based on a multireference PES for which all geomeries and frequencies of the relevant stationary points were optimized/calculated using complete active space self-consistent field (CASSCF) method with a polarized double-zeta Dunning−Hay basis set, and the energies were further determined by the internally contracted configuration interaction (ICCI) method with a Dunning correlation consistent triple-zeta double polarization atomic natural orbital basis set.[20] The assumption of disregarding two relatively smaller isomerization barriers was made[10] to simplify the complicated reaction mechanism.[18−20] According to the simplified *ab initio* PES diagram shown in Figure 1, the reaction mechanism of NH_2 with NO is depicted in the following scheme:

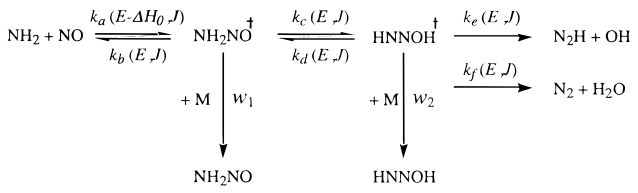

where "†" represents internal excitation. Here, ΔH_0 is the enthalpy difference between the reactants (NH_2 + NO) and the intermediate (NH_2NO) at 0 K, $k_i(E,J)$ is the microscopic rate coefficient at total energy E and total angular momentum J for the unimolecular dissociation or isomerization via corresponding channels (i = b, c, d, e, or f), and w_1 and w_2 are the effective quenching frequencies via collisional deactivation with a third body M for $NH_2NO^\dagger$ and $HNNOH^\dagger$, respectively. We thus modified Diau et al.'s steady-state formulas[10] to calculate the thermal rate coefficients of NH_2 with NO for each channel of the above mechanism with angular momentum conservation taken into account as follows:

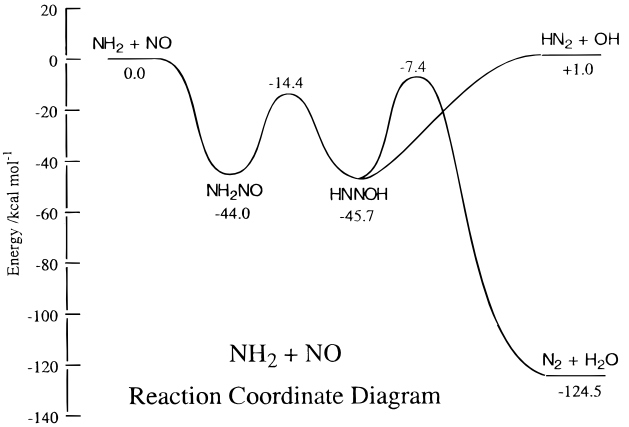

Figure 1. Potential energy surface diagram for the NH_2 + NO reaction based on the CASSCF/ICCI calculation.[20] The values represent relative energies in units of kcal mol^{-1} with zero-point energy corrections.

$$k_{rec}^{\infty}(T) = \frac{g_e}{hQ_r(T)} \sum_{j=0}^{\infty}(2J+1) \int dE\, W(E,J)\, e^{-E/k_BT} \quad (2)$$

$$k_{OH}(T) = \frac{g_e}{hQ_r(T)} \sum_{j=0}^{\infty}(2J+1) \int dE \frac{k_e(E,J)A(E,J)}{B(E,J)} W(E,J) e^{-E/k_BT} \quad (3)$$

$$k_{H_2O}(T) = \frac{g_e}{hQ_r(T)} \sum_{j=0}^{\infty}(2J+1) \int dE \frac{k_f(E,J)A(E,J)}{B(E,J)} W(E,J) e^{-E/k_BT} \quad (4)$$

$$k_{w_1}(T) = \frac{g_e}{hQ_r(T)} \sum_{j=0}^{\infty}(2J+1) \int dE \frac{w_1}{B(E,J)} W(E,J) e^{-E/k_BT} \quad (5)$$

$$k_{w_2}(T) = \frac{g_e}{hQ_r(T)} \sum_{j=0}^{\infty}(2J+1) \int dE \frac{w_2 A(E,J)}{B(E,J)} W(E,J) e^{-E/k_BT} \quad (6)$$

with

$$A(E,J) = k_c(E,J)/[k_d(E,J) + k_e(E,J) + k_f(E,J) + w_2]$$

and

$$B(E,J) = k_b(E,J) + k_c(E,J) + w_1 - k_d(E,J)A(E,J)$$

In eqs 2−6, h is Planck's constant, g_e is the electronic partition function ratio of the collision complex (assumed to be 1) with the reactants (2 for NH_2 and 2 + 2 $e^{-174/T}$ for NO), $Q_r(T)$ is the partition function of the reactants (electronic part and center of mass motion excluded), and k_B is Boltzmann's constant. w_1 and w_2 were calculated according to Troe's collision model[21] with the assumption of $\langle \Delta E \rangle$ = 1 kcal mol^{-1}, σ_{LJ} = 4 Å, and ϵ_{LJ} = 150 K for both intermediates colliding with Ar. The microscopic rate coefficients were determined by

$$k_i(E,J) = \frac{W_i(E,J)}{h\rho_j(E,J)}, \quad i = \text{b,c,d,e, or f}; \quad j = 1 \text{ or } 2 \quad (7)$$

where $W_i(E,J)$ is the sum of states of the corresponding transition state via channel i. Thus, we have $W(E,J) = W_b(E,J)$ and $W_c(E,J) = W_d(E,J)$. $\rho_j(E,J)$ is the density of states of the corresponding intermediate ($j = 1$ for NH_2NO and $j = 2$ for HNNOH) with $j = 1$ in case $i =$ b or c and $j = 2$ in case $i =$ d, e, or f.

$W_i(E,J)$ was evaluated in two different ways depending on the nature of the transition state (tight or loose). For a tight transition state ($i =$ c, d, or f), $W_i(E,J)$ was calculated by convolution of the sum of states of TSi with the derivative of one-dimensional tunneling probability function $P(\epsilon)$ for motion along the reaction coordinate:[23]

$$W_i(E,J) = \int_0^E \mathrm{d}\epsilon\, P'(\epsilon) W_i^{\ddagger}(E + V_{0,i} - \epsilon, J), \quad i=\text{c,d,or f} \quad (8)$$

where $W_i^{\ddagger}(E + V_{0,i} - \epsilon, J)$ is the convoluted rovibrational sum of states evaluated according to a modified Beyer−Swinehart algorithm[24] and $V_{0,i}$ is the barrier height of TSi with respect to the corresponding intermediate. For the case of the loose transition states (TSb or TSe) where there is no pronounced chemical barrier involved, μVTST theory[22] was implemented to determine the transition state variationally along the reaction coordinate. $W_i(E,J)$ is thus written as a convolution of the transitional-mode sum of states and the conserved-mode density of states $\rho_i^c(E^* - \epsilon)$:

$$W_i(E,J) = \int_{E_{\min}(J)}^{E^*} \mathrm{d}\epsilon\, \rho_i^c(E^* - \epsilon) W_i^{\mathrm{TM}}(\epsilon,J), \quad i=\text{b or e} \quad (9)$$

where $E_{\min}(J)$ is the minimum energy required to generate the angular momentum J, and E^* is the maximum energy available for distribution among the degrees of freedom orthogonal to the bond-length reaction coordinate r, determined by $E^* = E - V_i(r)$. Here $V_i(r)$ is the potential of the minimum energy pathway (MEP) on the potential surface with $i =$ b and e for $NH_2NO \rightarrow NH_2 + NO$ and $HNNOH \rightarrow HN_2 + OH$, respectively. However, both MEPs are not available currently according to recent *ab initio* data[18−20] owing to the difficulties of searching nonstationary points on the PES.[25,26] Therefore, a simple Morse-type function was used for both channels b and e:

$$V_i(r) = D_i[1 - \mathrm{e}^{-\beta_i(r-r_i)}]^2, \quad i =\text{b or e} \quad (10)$$

where D_i is the classical dissociation energy (zero-point energy excluded) for the breaking bond, r_i is the equilibrium bond length, and β_i is an empirical parameter for determining the slope of the MEPi. In eq 10, both D_i and r_i were fixed based on Walch's *ab initio* data,[20] but β_i was treated as a variable to be determined by fitting to the established room temperature experimental kinetic data. In fact, the rate coefficients of interest were not sensitive to β_i. Thus, a reasonable estimation for β_i was made for both MEPs with β_b and β_e equal to 2.0 and 3.0 $Å^{-1}$, respectively (see the following section for further discussion of this point).

The transitional-mode sum of states is classically evaluated using an analytic expression for the momentum−space volume and followed by Monte Carlo integration over the available configuration space of the four Euler angles. The accurate evaluation of this requires information about the anisotropy of the potential surface. We have used a simple model for this anisotropy in which the nonbonding interactions were treated by the Lennard-Jones 6-12 potential function with experimental pairwise parameters.[27] The anisotropy of the bonding potential was modeled by introducing a simple coupled $\cos^2\theta$ anisotropy factor as utilized by Wardlaw and Marcus for the methyl radical recombination,[28] modified for the reduced symmetry of the fragments in this case.[29,30] Twenty separations between 2.4 and 7.0 Å were employed for the μVTST calculations with all the relevant parameters summarized in the Appendix.

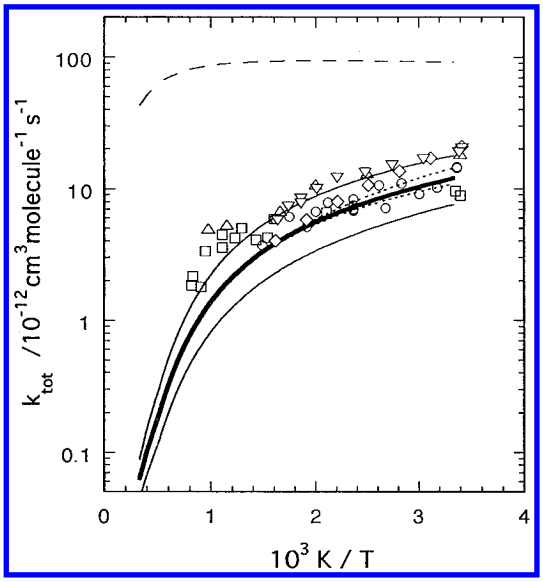

Figure 2. Arrhenius plots of the total rate coefficient (k_{tot}) for the NH_2 + NO reaction. The bold solid curve is the result of k_{tot} predicted by μVTST/RRKM theory using the original *ab initio* parameters without adjustments. The dotted and the plain solid curves are the sensitivity modeling results of k_{tot} using the same parameters as for the bold curve except changing β_b and D_b, respectively shown as former and latter curves (see text for more details). The symbols are the experimental data from different sources: (open suqares) Silver and Kolb;[5] (open diamonds) Bulatov et al.;[6] (open triangles) Atakan et al.;[7] (open reverse triangles) Wolf et al.;[9] (open circles) Diau et al.[10]

The total rate coefficient for the NH_2 + NO reaction is thus given by the sum of the individual thermal rate coefficients for all the open channels:

$$k_{tot} = k_{OH}(T) + k_{H_2O}(T) + k_{w_1}(T) + k_{w_2}(T) \quad (11)$$

and the branching ratio α is determined by

$$\alpha = k_{OH}(T)/k_{tot} \quad (12)$$

Results and Discussion

The μVTST/RRKM results are shown in Figures 2 and 3 for k_{tot} and α, respectively, in comparison with the most recent experimental data. In Figure 2, the long-dashed curve is the capture rate coefficient for the recombination of NH_2 with NO under high-pressure-limiting conditions (eq 2), and the bold solid curve is the result of k_{tot} obtained from eqs 3−6 and eq 11, both curves computed using the RRKM parameters listed in the Appendix based on Walch's *ab initio* result without further modifications. The predicted k_{tot} decreases dramatically with increasing temperature, especially for temperatures higher than 1000 K owing to the significant contribution of back-dissociation of $NH_2NO^{\dagger}$ to form NH_2 + NO.

As mentioned in the previous section, the lack of accurate *ab initio* data for both bond-fission channels necessitated the use of the crude model potentials for the MEPs as well as the bonding and nonbonding interactions to evaluate the sum of states for the transitional modes. Thus, we have carried out a simple sensitivity test for the Morse potentials employed by varying the key empirical parameters introduced in eq 10. From the potential energy diagram of Figure 1, it is apparent that the reaction 1a is nearly thermoneutral and reaction 1b has no intrinsic barrier relative to NH_2 + NO. Hence, k_{tot} is expected to be most sensitive to the parameters of TSb, especially the MEP. The dotted curves shown in Figure 2 are the results

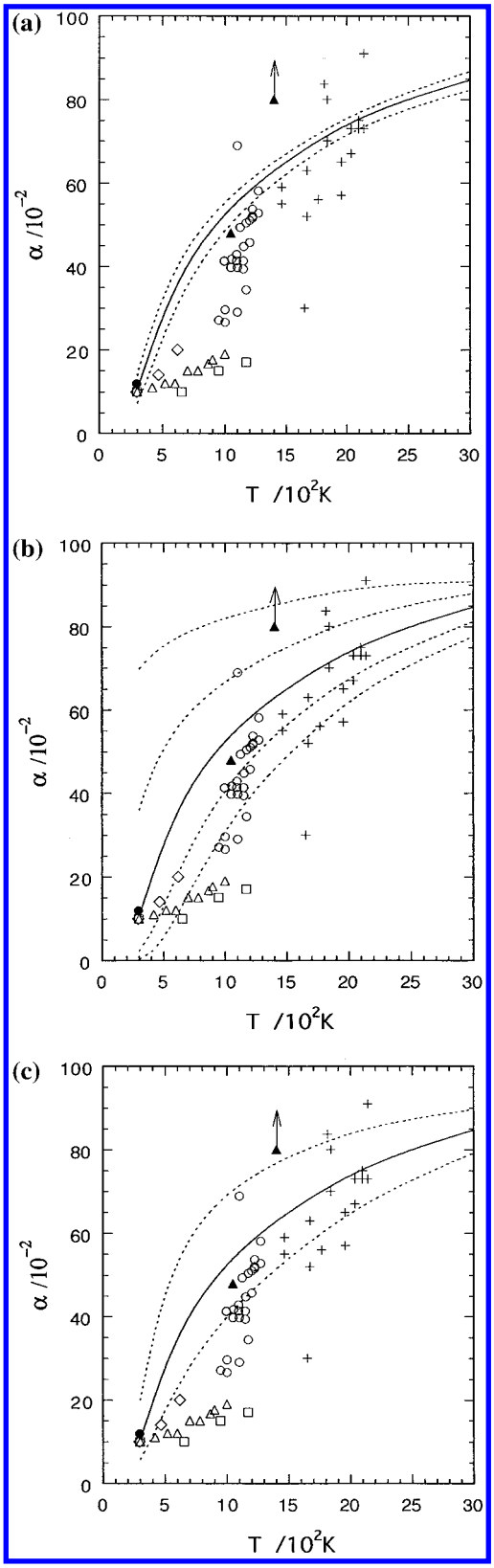

Figure 3. Temperature dependence of the branching ratio (α) for the NH_2 + NO reaction. The solid curves shown in parts a−c are the same results of α obtained from μVTST/RRKM calculations using the original *ab initio* parameters without adjustments. The dotted curves are the sensitivity modeling results of α using the same parameters as for the solid curves except changing β_e, the enthalpy of reaction 1a, and the relative energy of TSf, respectively shown in parts a−c (see text for more details). The symbols are the experimental data from different sources: (filled circles) Silver and Kolb;[5] (open diamonds) Bulatov et al.;[6] (open triangles) Atakan et al.;[7] (open squares) Stephens et al.;[8] (filled triangles) Kimball-Linne and Hanson;[11] (crosses) Vandooren et al.;[12] (open circles) Halbgewachs et al.[13] The upward arrow represents a lower limit prediction.

obtained using the same parameters as for the bold solid curve, except that the value of β_b is changed from the optimum value required to fit the well-established room temperature experimental data (2.0 $Å^{-1}$) to β_b = 1.5 and 2.5 $Å^{-1}$, respectively, for the upper and lower curves. We find that the total rate is relatively insensitive to β_b, which lends a certain amount of confidence to the trends observed in the absence of accurate *ab initio* data for the MEP. In order to estimate the possible effect of using different functional forms for the model MEP, we have carried out the same procedure of fitting the beta parameter to ensure a match with the room temperature kinetic data, but with a Varshni rather than a Morse potential. The results lay within 3% of the solid line obtained with the optimum Morse potential and so have not been independently plotted. The plain solid curves shown in Figure 2 are the results obtained by changing the value of the bond dissociation energy D_b by +2 kcal mol^{-1} (upper curve) and −2 kcal mol^{-1} (lower curve) with respect to the *ab initio* value of 51.6 kcal mol^{-1} (ΔH_0 = 44.0 kcal mol^{-1}). The calculations for k_{tot} are in excellent agreement with those of Diau et al.[10] (open circles) for the entire temperature range of their study (297−673 K) and indeed provide a quite acceptable representation of the temperature dependence implied by the other experimental data also, within reasonable error bounds associated with uncertainties in the PES parameters.

There has not been any experimental observation of ΔH_0 for the formation of NH_2NO reported in the literature. Our calculations indicate that the collisional deactivation of both $NH_2NO^\dagger$ and $HNNOH^\dagger$ intermediates is negligible (<2%) for the entire temperature range (300−3000 K) under 50 Torr of Ar, in accordance with the conclusion of Diau et al.[10] and Phillips.[17] This implies the difficulty of observing NH_2NO under normal experimental conditions (NH_2NO might be observed under matrix-isolated conditions, but it would be very hard to measure the ΔH_0). The quantum-mechanical tunneling corrections incorporated for TSc/d and TSf are negligible in this study owing to the fact that the barriers for the tight transition states are well below the threshold for formation of the collision complexes from reactants NH_2 and NO (−14.4 and −7.4 kcal mol^{-1} for TS c/d and f, respectively).

We now discuss the controversial parameter α. As one may notice from the scattered experimental points in Figure 3, there exist significant discrepancies between direct measurements of α at lower temperatures and values inferred indirectly from kinetic modeling at higher temperatures. The results of our μVTST/RRKM calculations, obtained via eq 12 and the related equations using the relevant parameters listed in the Appendix, are indicated by the solid curves shown in Figure 3. The predicted values for α are found to be strongly temperature dependent, increasing rapidly from 0.1 at room temperature to 0.85 at 3000 K. Recall that we have fit α and k_{tot} at room temperature in order to obtain estimates for the Morse beta parameters for the entrance channel and the OH exit channel. Hence, the agreement at room temperature is by design. However, no further modification of parameters is involved at higher temperatures. Hence, the rapid increase of α with temperature is a genuine prediction. Although the high-temperature flame modeling data are somewhat scattered, it is clear that our calculations are broadly consistent with the rapid increase in the branching ratio that is inferred by these data. A much slower increase of α with temperature in the range 300−1000 K is suggested by the direct laser kinetic data of Atakan et al.[7] (open triangles) and Stephens et al.[8] (open squares). If their data are correct, an almost step-like temperature dependence of α would be implied. According to the results of kinetic modeling and sensitivity analysis, however, Diau et al.[10] pointed

TABLE 1: Relative Energies, Vibrational Frequencies, and Moment of Inertia for the NH_2 + NO Reaction[a]

	NH_2	+	NO	NH_2NO	TSc, TSd	TS_f	HNNOH	HN_2	+	OH
					Relative Energies					
ΔE^b		0.0		−44.0	−14.4	−7.4	−45.7		1.0	
					Vibrational Frequencies					
ω_1	3287			3871	3791	4030	3660			3624
ω_2	3239			3490	2160	3688	3313	2744		
ω_3			1943	1792	1642	1793	1623	1583		
ω_4	1528			1709	1562	1194	1466			
ω_5				1368	1348	595	1405	1070		
ω_6				1207[c]	1006	389	912[c]			
ω_7				712	1207	576	652			
ω_8				647	629	344	959			
ω_9				542	1990*i*	1359*i*	509			
					Moment of Inertia					
A	23.528			2.669	2.416	2.455	2.504	21.402		
B	13.013		1.704	0.436	0.504	0.356	0.416	1.499		18.203
C	8.379			0.378	0.417	0.311	0.357	1.401		

[a] All values are in units of cm^{-1} except for those of energies in kcal mol^{-1}. [b] Zero-point energy corrections included. [c] Vibrational modes related to the corresponding reaction coordinates.

out that the latter study might involve serious secondary reactions such as $NH_2 + H \rightarrow NH + H_2$ and $NH_2 + NH_2 \rightarrow NH + NH_3$.

It is necessary to consider the effect of changing the PES parameters used in our calculations within expected uncertainty bounds. The aforementioned sensitivity of k_{tot} on D_b (or ΔH_0) does not hold similarly for α owing to its evaluation as the *ratio* of k_{OH} to k_{tot}. Instead, the parameters for the competitive channels of TSe and TSf will be the dominant factors in determining α. In order to investigate the sensitivitiy of α to these parameters, we have carried out a series of calculations indicated in Figure 3. In Figure 3a, the effect of modifying the Morse parameter β_e was modeled by varying the values from 2.5 (upper dotted curve) to 3.5 $Å^{-1}$ (lower dotted curve) with respect to our estimated value, 3.0 $Å^{-1}$ (solid curve). We observe little sensitivity to this parameter. Next, the effect of modifying the enthalpy of reaction 1a by changing the value for the ground-state energy of the N_2H + OH fragments calculated by Walch is considered. In Figure 3b, the four dotted curves are, from top to bottom, the calculated values for α with the enthalpy of reaction 1a shifted from its predicted value of 1 kcal mol^{-1} [20,31] by −2, −1, +1, and +2 kcal mol^{-1}, respectively. Although not unexpected,[10] it is certainly noteworthy (and sobering) to see such large changes in the predicted values for this rather critical branching ratio by varying the enthalpy of reaction 1a within a fairly typical uncertainty range for *ab initio* calculations, ±2 kcal mol^{-1}. Finally, in Figure 3c, the effect of modifying the barrier height for TSf on the predicted temperature dependence of α is indicated. The dotted curves in Figure 3c show the predictions for α when the barrier height of TSf is varied by −2 kcal mol^{-1} (lower curve) and +2 kcal mol^{-1} (upper curve) with respect to the raw *ab initio* value (−7.4 kcal mol^{-1} relative to the reactants). The results illustrated in Figure 3 show that both the ground-state energy of the N_2H + OH pair and the height of the barrier for TSf play very important roles in determining the branching ratio α under combustion conditions, but the former has a larger effect than the latter.

Conclusion

Recently, Glarborg et al.[3,4] proposed an expression for the branching ratio α as a function of temperature with two empirical parameters:

$$\alpha = CT^n \tag{13}$$

where *C* was chosen so that α =0.12 at 300 K. They have shown that a value of $n > 0.7$ is required in order to successfully model their flow reactor data under thermal $DeNO_x$ temperatures. Contrastingly, a value for $n < 0.4$ would be required to fit the data of Atakan et al.[7] and Stephens et al.[8] with eq 13. We illustrated in Figures 2 and 3 above the new predictions provided by our μVTST/RRKM calculations and also the sensitivity of these predictions to certain critical PES parameters. Regardless of the particular combination of parameters chosen, our calculations show one consistent trend—that the branching ratio α for formation of OH increases strongly with temperature such that the OH product channel becomes dominant at higher temperatures, and it is this conclusion that is the main result of the present study. Our results are consistent with, and provide support for, the temperature dependence of α proposed by Miller and Glarborg[4] for use in kinetic modeling under combustion conditions.

It is interesting to speculate on the cause of the dramatic increase in α with temperature. In particular, one expects that angular momentum may play an important role in the effect because the rate-determining step for water formation occurs via a "tight" transition state at a chemical barrier, whereas the rate-determining step leading to formation of OH occurs via a "loose" transition state.[34] These two qualitatively different types of transition state are known to be subject to quite different energetic constraints as angular momentum increases, owing to the presence in the former case and the absence in the latter of a pronounced centrifugal barrier.[24,35,36] Further characterization of the temperature dependence of the NH_2 + NO reaction, and testing of such speculations, will clearly require improved *ab initio* calculations of the potential energy surface parameters. We are currently pursuing this objective within the context of a more detailed study.[37]

Acknowledgment. This work has been carried out with the support of the Australian Research Council Large Grants Scheme (Grant No. A29532744). We are grateful to Drs. J. Durant and J. A. Miller for helpful discussions.

Appendix

The μVTST/RRKM parameters of the NH_2 + NO reaction for the reactants, products, intermediates, and transition states are summarized in Table 1, based on Walch's CASSCF/ICCI calculations.[20,31,32] The details of getting relevant parameters

to evaluate the sum of states for the TSb and TSe according to eq 9 are described as follows.

$$NH_2NO \xrightarrow{TSb} NH_2 + NO \qquad (a)$$

The vibrational frequencies of the reactants (NH_2 + NO) shown in Table 1 were obtained by slightly scaling with a factor of 1.02 from the experimental values[33] based on the zero-point energy reported in ref 20, and the moment of inertia were adopted from the experimental data.[33] The MEPb was modeled by eq 10 with D_b, r_b, and β_b equal to 51.6 kcal mol^{-1}, 1.344 Å, and 2.0 Å^{-1}, respectively. The sum of states of TSb was evaluated based on 20 points between 2.4 and 7.0 Å for the N−N bond separation along the reaction coordinate r. The conserved-mode density of states was evaluated using the vibrational frequencies obtained by interpolating between the vibrational frequencies of the reactants (ω_1, ω_2, and ω_4 for NH_2 and ω_3 for NO) and those corresponding to the intermediate (NH_2NO) along the reaction coordinate r. The similar interpolation procedure was also employed to obtain the reference geometries of the two fragments (NH_2 and NO) with the separation distances of 2.4−7.0 Å along the reaction coordinate for the transitional-mode sum of states calculations. All interpolation procedures were based on a simple exponential function[28] with an empirical factor of 1.3 Å^{-1}.[38]

$$HNNOH \xrightarrow{TSe} HN_2 + OH \qquad (b)$$

The vibrational frequencies and moment of inertia of HN_2 and OH shown in Table 1 were cited from Walch's earlier work[31,32] in consistency with the present study. The Morse parameters D_e, r_e, and β_e were set to 48.9 kcal mol^{-1}, 1.404 Å, and 3.0 Å^{-1}, respectively. All the other procedures of getting interpolation parameters for evaluation of the sum of states of TSe by eq 9 are similar to those of TSb mentioned previously.

For both TSb and TSe, the nonbonding interactions between two fragments (bonding atom pairs excluded) were modeled by a Lennard-Jones potential given by $4\epsilon[(\sigma/d)^{12} - (\sigma/d)^6]$, where d represents the distance between the nonbonding atom pairs with the homogenous pairwise parameters (σ /Å, ϵ /cm^{-1}) assigned to be (2.81, 5.89), (3.31, 25.9), and (2.95, 42.8) for the H−H, N−N, and O−O pairs, respectively.[27] By use of the venerable Lorentz−Berthelot mixing rules,[27] interactions between unlike atoms were approximated with the pairwise parameters of (3.06, 12.4), (2.88, 15.9), and (3.13, 33.3) for the H−N, H−O, and N−O pairs, respectively.

References and Notes

(1) Miller, J. A.; Branch, M. C.; Kee, R. J. *Combust. Flame* **1981**, *43*, 81.

(2) Miller, J. A.; Bowman, C. T. *Prog. Energy Combust. Sci.* **1989**, *15* , 287.

(3) Glarborg, P.; Dam-Johansen, K.; Miller, J. A.; Kee, R. J.; Coltrin, M. E. *Int. J. Chem. Kinet.* **1994**, *26*, 421.

(4) Miller, J. A.; Glarborg, P. *Gas Phase Chemical Reaction Systems: Experiments and Models 100 Years after Max Bodenstein*; Springer Series in Chemical Physics, in press.

(5) (a) Silver, J. A.; Kolb, C. E. *J. Phys. Chem.* **1982**, *86*, 3240. (b) Silver, J. A.; Kolb, C. E. *J. Phys. Chem.* **1987**, *91*, 3713.

(6) Bulatov, V. P.; Ioffe, A. A.; Lozovsky, V. A.; Sarkisov, O. M. *Chem. Phys. Lett.* **1989**, *161*, 141.

(7) Atakan, B.; Jacobs, A.; Wahl, M.; Weller, R.; Wolfrum, J. *Chem. Phys. Lett.* **1989**, *155*, 609.

(8) Stephens, J. W.; Morter, C. L.; Farhat, S. K.; Glass, G. P.; Curl, R. F. *J. Phys. Chem.* **1993**, *97*, 8944.

(9) Wolf, M.; Yang, D. L.; Durant, J. L. *J. Photochem. Photobiol., A* **1994**, *80*, 85.

(10) Diau, E. W.; Yu, T.; Wagner, M. A. G.; Lin, M. C. *J. Phys. Chem.* **1994**, *98*, 4034.

(11) Kimball-Linne, M. A.; Hanson, R. K. *Combust. Flame* **1986**, *64*, 337.

(12) Vandooren, J.; Bian, J.; van Tiggelen, P. J. *Combust. Flame* **1994**, *98*, 402.

(13) Halbgewachs, M. J.; Diau, E. W. G.; Mebel, A. M.; Lin, M. C.; Melius, C. F. *26th Symposium (International) on Combust.ion*; The Combustion Institute: Pittsburgh, PA, submitted.

(14) Gilbert, R. G.; Whyte, A. R.; Phillips, L. F. *Int. J. Chem. Kinet.* **1986**, *18*, 721.

(15) Casewit, C. J.; Goddard, W. A., III. *J. Am. Chem. Soc.* **1982**, *104*, 3280.

(16) Abou-Rachid, H.; Pouchan, C.; Chaillet, M. *Chem. Phys.* **1984**, *90*, 243.

(17) Phillips, L. F. *Chem. Phys. Lett.* **1987**, *135*, 269.

(18) Melius, C. F.; Binkley, J. S. *20th Symposium (International) on Combustion*; The Combustion Institute: Pittsburgh, PA, 1985; p 575.

(19) Harrison, J. A.; Maclagan, G. A. R.; Whyte, A. R. *J. Phys. Chem.* **1987**, *91*, 6683.

(20) Walch, S. P. *J. Chem. Phys.* **1993**, *99*, 5295.

(21) Troe, J. *J. Phys. Chem.* **1979**, *83*, 114.

(22) (a) Smith, S. C. *J. Chem. Phys.* **1991**, *95*, 3404. (b) Smith, S. C. *J. Chem. Phys.* **1992**, *97*, 2406. (c) Smith, S. C. *J. Phys. Chem.* **1993**, *97*, 7034. (d) Smith, S. C. *J. Phys. Chem.* **1994**, *98*, 6496.

(23) Miller, W. H. *J. Am. Chem. Soc.* **1979**, *101*, 6810.

(24) Gilbert, R. G.; Smith, S. C. *Theory of unimolecular recombination reactions*; Blackwell Scientific Publication: Carlton, Australia, 1990.

(25) Stanton, J. F. *J. Chem. Phys.* **1994**, *101*, 371.

(26) Chen, W.; Schlegel, H. B. *J. Chem. Phys.* **1994**, *101*, 5957.

(27) Allen, M. P.; Tildesley, D. J. *Computer Simulation of Liquids*; Oxford Science Publications: Clarendon Press, Oxford, 1987; p 21, and references therein.

(28) (a) Wardlaw, D. M.; Marcus, R. A. *J. Chem. Phys.* **1985**, *83*, 3462. (b) Wardlaw, D. M.; Marcus, R. A. *J. Phys. Chem.* **1986**, *90*, 5383.

(29) Guo, Y.; Smith, S. C.; Moore, C. B.; Melius, C. F. *J. Phys. Chem.* **1995**, *99*, 7473.

(30) Klippenstein, S. J.; Marcus, R. A. *J. Chem. Phys.* **1989**, *91*, 2280.

(31) Walch, S. P.; Duchovic, R. J.; Rohlfing, C. M. *J. Chem. Phys.* **1989**, *90*, 3230.

(32) Walch, S. P. *J. Chem. Phys.* **1993**, *98*, 1170.

(33) Chase, M. W., Jr.; Davies, C. A.; Downey, J. R., Jr.; Frurip, D. J.; McDonald, R. A.; Syverud, A. N. JANAF Thermochemical Tables. *J. Phys. Chem. Ref. Data* **1985**, *14*.

(34) Miller, J. A. Private communication.

(35) Smith, S. C.; Gilbert, R. G. *Int. J. Chem. Kinet.* **1988**, *20*, 979.

(36) Troe, J. *Adv. Chem. Phys.* **1992**, *82*, 485.

(37) Diau, E. W.-G.; Smith, S. C.; Hu, C.-H.; Schaefer, H. F., III; Yang, D. L.; Durant, J. L., Jr. Work in progress.

(38) Based on the value for the NO_2 system cited in ref 28.

JP9602991